Advances in Science and Technology Research Journal

Advances in Science and Technology Research Journal 2024, 18(3), 1–13
https://doi.org/10.12913/22998624/185394
ISSN 2299-8624, License CC-BY 4.0

Received: 2024.01.15
Accepted: 2024.02.26
Published: 2024.04.20

Susceptibility to Stress Corrosion Cracking of Selected Amorphous Polymer Materials in a Seawater Environment

Monika Chomiak[1*], Małgorzata Szymiczek[1], Sara Sarraj[1]

[1] Department of Theoretical and Applied Mechanics, Faculty of Mechanical Engineering, Silesian University of Technology, ul. Konarski 18A, 44-100 Gliwice, Poland

* Corresponding author's e-mail: monika.chomiak@polsl.pl

ABSTRACT

This paper aimed to determine the susceptibility of polycarbonate and polymethylmethacrylate to corrosion cracking under specific operating conditions. The tests included static tensile and flexure, impact strength, and microscopic examination. Due to the synergistic effect of tensile stresses and seawater environment, numerous cracks are observed. Moreover, aging conditions did not significantly reduce the strength properties of the tested specimens; thus, higher resistance to stress corrosion cracking does not have a close relationship with the material's mechanical properties.

Keywords: aging, thermoplastic, polycarbonate, polymethylmethacrylate, mechanical tests

INTRODUCTION

Stress corrosion cracking (SCC) is a phenomenon that plays an important role in the degradation of materials. It is a phenomenon consisting of the destruction of polymer elements (cracking) caused by internal stresses (due to processing) or stresses forced by external loads. The mechanism of stress corrosion cracking is complex and often related to the structure of the material. Mechanisms of loading specimens during flexural are widely described in the literature, where the use of appropriate supports enables tests with different loading conditions – two-point, three-point, and four-point flexural. The described loading systems are taken from stress corrosion tests for metals and their alloys (EN ISO 7539-1:2013-06). There are also U-bend and C-bend solutions [1, 2]. The tensile loading method adopted in this study which allows for minimizing the influence of gravity, is unique.

Long-term load operation (also with low values) in the conditions of an active (aggressive) environment or elevated temperature may initiate slow damage to the structure of the material leading to the destruction of the elements [3]. It is one of the main threats to the durability and safety of various structures, including bridges, pipelines, ships, and aircrafts [4, 5]. Environmental stress cracks may account for approximately 15–30% of all failures of exploitation polymer components. Research also shows that stress cracking does not break polymer bonds, but only breaks secondary connections between polymers. Material destruction resulting from stress corrosion cracking is the result of mechanical stress causing small cracks that quickly spread in difficult environmental conditions [6]. Few methods have been recently introduced to account for the quantitative fracture analysis [7].

This phenomenon can also be seen in plastics. In addition to the effects of chemical factors, which can lead to softening or plasticization, there are also purely physical processes, such as diffusion, swelling, and cross-linking, manifested by the occurrence of stress corrosion cracking in these materials. The occurrence of stress corrosion cracking is not unique to all polymeric materials. However, it largely depends on factors such as chemical structure, bonding, crystallinity, surface

roughness, molecular weight, and residual stresses of the polymer. It also depends on the chemical structure and concentration of the liquid reagent, the temperature of the system, and the strain rate.

Scientists indicate the need to conduct research related to the occurrence of stress corrosion cracking in polymeric materials to assess the reliability of their operation under specific conditions. Research conducted by T. Kawaguchi et al., [8] showed that for ABS (acrylonitrile-butadiene-styrene), crack propagation caused by stress corrosion cracking occurs at room temperature under the influence of non-ionic surfactants. P. Dunn et al., [9] showed that polyamide does not show a significant relationship between crack propagation and loading speed. In the case of aging, creep or relaxation is often observed, which is related to the influence of a state of stress or deformation. In addition, the action of heat affects the creep of materials. The phenomenon of stress corrosion cracking also applies to popular polymer composite materials reinforced with glass fiber. Recently, many scientific articles [9–11] have been carried out to determine the susceptibility of these materials to corrosion under various test conditions. Ramos E. and Kumosa M. [11] investigated the synergistic effects of exposure to nitric acid, elevated temperature, and applied bending stresses on the stress corrosion cracking of vinyl ester-epoxy matrix glass composites for boron-free and traditional fibers. The synergistic effect was found to be much stronger on stress corrosion cracking than the effect of individual factors.

Research was carried out on thermoplastics and polymer composites based on resins [12–27]. To name several examples, SCC can be observed when exposing polyethylene to aqueous detergents or organic solvents [24], high impact polystyrene to sunflower oil [25], the stress cracking behavior of injection moulded PET was investigated using sodium hydroxide (NaOH) aqueous solutions in various concentrations as active fluids [26], polycarbonate to ethanol or fat emulsions [27]. The conducted research aims to determine the influence of environmental factors, i.e. temperature and water salinity, on the speed and intensity of stress corrosion cracking of selected amorphous thermoplastic polymer materials in the form of plates produced by extrusion. The obtained test results allow predicting the time of failure-free operation in the tested operating conditions of products made of the tested polymer materials.

MATERIALS AND METHODS

Tested materials

Two amorphous polymeric materials plates made of polymethylmethacrylate (PMMA) Turcyl, Q 3 mm thick, (Tuplex Ltd., Gliwice, Poland) [28] and polycarbonate (PC) Exonol 3 mm thick (Exolon Group GmbH, Munich, Germany) [29] were selected for the tests due to their specific properties (shown in Table 1 and Table 2) and their use (Table 3) in elements in contact with the research environment, such as seawater. Polycarbonate is a widely used and susceptible material to environmental stress cracking (ESC) from a variety of fluids. The specimens for stress corrosion tests had the shape of a beam with dimensions of 250×50×3 mm. Test specimens in the shape of flat bars were prepared by machining methods. Each specimen was mounted in a separate tensile fixture.

The materials used in the research are used for elements in contact with seawater. PC is used for float switches designed to control or signal the liquid level in open and closed tanks. It is an element in contact with an aggressive environment - in this case seawater, PMMA in turn, is a material that perfectly transmits light and can be used as a solution for viewing panels in seawater tanks in the Gansky Africarium. These tanks can have a structure made of PMMA (Z10 jellyfish tank) or be made entirely of PMMA (Z11 “shoe” tank) [30–32].

PMMA and PC are materials that are undoubtedly used in many fields and industries, also in the environment of salty seawater.

Both materials – PC, and PMMA are entirely resistant to seawater. It was found that PC is resistant to higher temperatures than PMMA because its heat distortion temperature is 135 °C, whereas PMMA withstands only up to 95 °C [28–29].

Research methodology of stress corrosion cracking

The stress corrosion cracking studies research station was designed and equipped to allow for precise temperature regulation, the accommodation of three tensioning systems, and the ability to withstand harsh environmental conditions.

Device for carrying out stress corrosion of polymeric materials are not popular in the world of science, but there have been few studies on stands adapted for this purpose [36]. The lack of

Table 1. Selected properties of tested materials based on [28–29, own research]

Properties	Type of property	PMMA	PC
Mechanical	Density (method D, E, ISO 1183-1:2019), g/cm^3	1,18	1,2
	Stress at break (ISO 527-1:2020-01), MPa	42	67
	Strain at break (ISO 527-1:2020-01), %	4,5	124
	Flexural strength (ISO 178:2019-06), MPa	76	96
	Impact strength PN-EN ISO 179-1:2023-11 (+23°C), kJ/m^2	1,11	71
	Shore`a D hardness (PN-EN ISO 868:2005), ShD	80	83,5
Thermal	Melting point (method A, ISO 3146:2022-09), °C	103	=
	Heat deflection temperature (method A, ISO 75-1:2020-09), °C	95	135
	Heat deflection temperature (method B, ISO 75-1:2020-09), °C	100	142

Table 2. Chemical resistance of the tested materials to selected chemical compounds based on [33–35]

	Compound	PMMA	PC	
Environmental resistance at 60 °C	Nitric acid 50%	0	0	(-) no chemical resistance. (0) conditional chemical resistance. (+) total chemical resistance.
	Chlorine	-	-	
	Bromine	-	-	
	Hydrochloric acid	-	-	
	Sodium chloride	+	+	
	Calcium chloride	+	+	
	Magnesium chloride	+	+	
	Iodine/potassium iodide (solution)	-	-	
	Seawater in 23 °C	+	+	
	Pyridine	-	-	
	Xylene	-	-	
	Acetone	-	-	

Table 3. Examples of applications of the tested materials [31, 36]

	PMMA	PC
Application	- glazing: roof slope, advertising space, doors, and windows, partition walls, paintings, greenhouses and winter gardens, showcases, and shop displays - decorative elements of stands, - acoustic screens, protective screens, sound barriers, - viewing panels in seawater tanks used, e.g., in Africarium Gansky	- in the production of anti-burglary covers, - as small partition walls, - as safe glazing of doors or windows, - in the construction of orangeries and small gazebos, - in the construction of acoustic screens, - in the construction of machine and cabin covers.

ready-made devices for testing the phenomenon of stress corrosion of polymeric materials on the market has resulted in the need to prepare a stand dedicated to this type of research and develop research methodology. The tests were carried out on an original laboratory stand [38], the construction of which allows the testing of specimens in a specific range of geometry for constant or variable loads and in any simulated operating conditions (Fig. 1). The construction of the test stand allows stress to be exerted in the tested object by constant load or permanent displacement. The station's desktop allows control of the temperature of the fluid inside the tank. The proposed solution allows to minimize the influence of gravity on the loaded specimens. The research station (Fig. 1) consists of the following components.

Table 4 is the composition of seawater based on ASTM D1141-52. The temperature applied in the tests was 65±2 °C, and salinity of seawater 3.5$^{o}/_{oo}$. Pneumatic pressure was 5.5 bar, so the tensile force was about ¼ of the yield stress. A calculator dedicated by Pneumatig company was used to properly convert air pressure into stress in

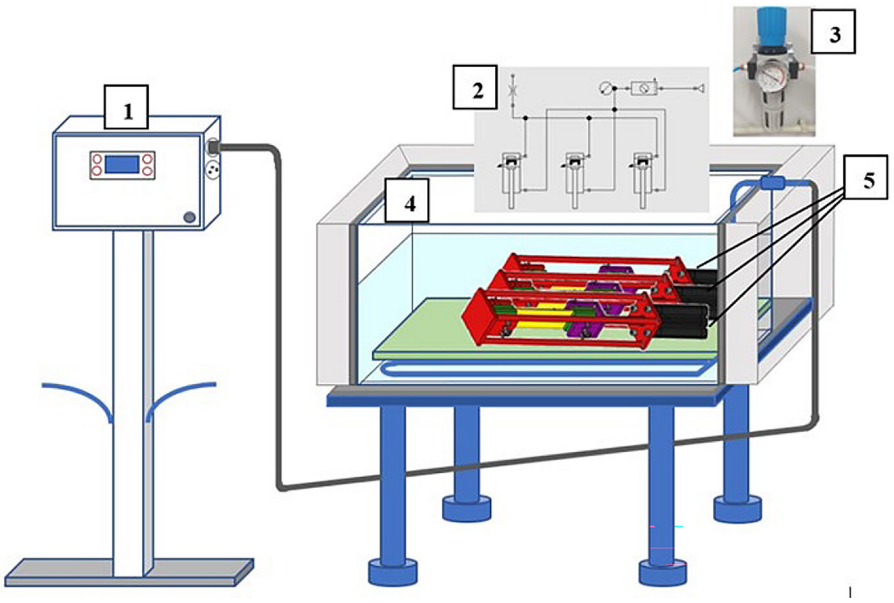

Figure 1. Research station diagram: (1) control cabinet, (2) pneumatic supply diagram, (3) pressure regulator, (4) specimen tank filled with test solution, (5) tensile grips with the specimen

Table 4. Substitute seawater composition based on ASTM D1141-52

Substitute	Quantity (g/l)
NaCl	24.5300
$MgCl_2$	5.2000
$CaCl_2$	1.1600
Na_2SO_4	4.0000
KCl	0.6950
$NaHCO_3$	0.2010
KBr	0.1010
H_3BO_3	0.0270
$SrCl_2$	0.0250
NaF	0.0030

the specimen. Three specimens of each material were prepared and tested in two separate cycles. Each specimen was mounted in a separate tensile grip, and then the entire system was immersed in water. The test time for PMMA was 120 h = 1825 days (5 years), and for PC was about 24 h = 365 days (1 year) for mean temperature seawater in the Baltic Sea is 11 °C [37]. For the purpose of this paper, specimens subjected to stress corrosion crack simulation process will be described as aged specimens.

The assessment of the impact of specific conditions on properties was made based on the following:

- static tensile test according to ISO 527 -1:2020-01,
- flexural strength according to ISO 178 :2019-06,
- the Charpy impact strength by ISO 179 -2:2020-12,
- hardness according to ISO 868:2005,
- density according to ISO 1183-1:2019-05,
- examination with a stereoscopic microscope,
- fourier transform infrared spectroscopy (FTIR).

Tensile test

The static tensile test was carried out on the Shimadzu kN10D machine cooperating with the TRAPEZIUMX-V software. The traverse speed was 20 mm/min. Strength tests were carried out on 5 reference specimens of both tested materials and 5 specimens of PMMA and PC after the tests stress corrosion cracking. The specimens were prepared by ISO 527-2:2012 type BA. Based on the obtained results, the following were determined tensile strength and strain at break.

Three-point flexural test

A static three-point flexural test according to ISO 178:2019-06 was carried out on the Shimadzu kN10D machine cooperating with the TRAPEZIUMX-V software. The traverse speed was 5 mm/min. Strength tests were carried out on 5 reference specimens of both tested materials and 5 specimens of PMMA and PC after the tests stress

corrosion cracking. The specimens were prepared by ISO 178:2019-06 method B. Based on the obtained results, the flexural strength, flexural modulus, and flexural deformation were determined.

Impact test

The notched Charpy impact strength was determined by ISO 179-2:2020-12 using a Charpy pendulum impact tester HIT5.5P produced by Zwick Roell company. The 80×10×4 mm specimens were V-notched on a special device, ensuring the results' repeatability. Charpy notched impact strength was carried out on 10 reference specimens of both tested materials and for 10 specimens of PMMA and PC after the tests stress corrosion cracking.

Shore D hardness analysis

Hardness measurements were carried out by ISO 868:2005 using a Shore-type D hardness tester. The test was repeated five times, maintaining a distance of at least 10 mm from the edge.

Density

The density of tested materials was determined using an analytical balance equipped with a hydrostatic density measurement kit (Ohaus Adventurer Pro, OHAUS Europe GmbH, Greifensee, Switzerland) following the standard ISO 1183-1:2019-05. The test was carried out on three specimens of each material with dimensions 20×20×3 mm.

Structure study

Microscopic examination of the structure of the specimens was carried out using a ZEISS SteREO Discovery.V12 stereoscopic microscope. The specimens before microscopic examination were cleaned of sediments of left sea salt with water.

Fourier transform infrared spectroscopy

The changes occurring in the structure of the tested materials after corrosion tests were assessed based on their IR spectra. The analysis was performed using an FTIR spectrophotometer (Shimadzu Corporation, Kyoto, Japan) attenuated total reflection mode. Spectra were collected over the mid-infrared range with a resolution of 2 cm^{-1} and 20 scans.

RESEARCH RESULTS

Stress corrosion test results

Based on the tests carried out and Arrhenius law, it is possible to predict the durability of the tested materials in aggressive conditions at constant stress. The assumed test time and conditions result from the adopted application.

The results of the strength tests clearly show that the strength properties of the tested specimens before and after aging do not show significant differences, which means that the specific test environment does not have a negative impact on the tested properties (Fig. 3–9). On the surface of all specimens, cracks were noticeable, as shown in Figure 10–12. The cracks on PMMA were smaller, but there were much more of them than on PC. Most of the minor corrosion cracks occurred in the grip rea.

Tensile test results

Figure 2 shows the stress-strain curve of PMMA (a) and PC (b). Figure 3 shows the change in tensile strength with respect to aging time for the tested materials. Analyzing the graph (Fig. 3), it can be seen that the PC and PC_S specimens have practically identical tensile strength, almost twice that of the PMMA and PMMA_S specimens. PMMA has a higher tensile strength than PMMA_S specimens. The differences between the tensile strength for unaged PC and PMMA are approximately 38%, while after exposure to the assumed tensile force and temperature it increases to approximately 47%. Different effects of test conditions on the behavior of materials are observed. It should be noted that the time of the corrosion test was a very important condition. The tensile strength of PC specimens before and after aging was almost the same. Only a larger standard deviation was observed, which is probably related to the given load condition. The tensile force generates tensile stresses, and the molecules also stretch. However, with such short duration of force exposure, structural changes vary in the specimen subjected to stress corrosion testing, from which specimens were then cut to determine the tensile strength. The tensile strength of PMMA after corrosion testing decreased by approximately 14%, but the dispersion of the results decreased. This is probably related to the impact of the corrosive environment and load. PMMA is characterized

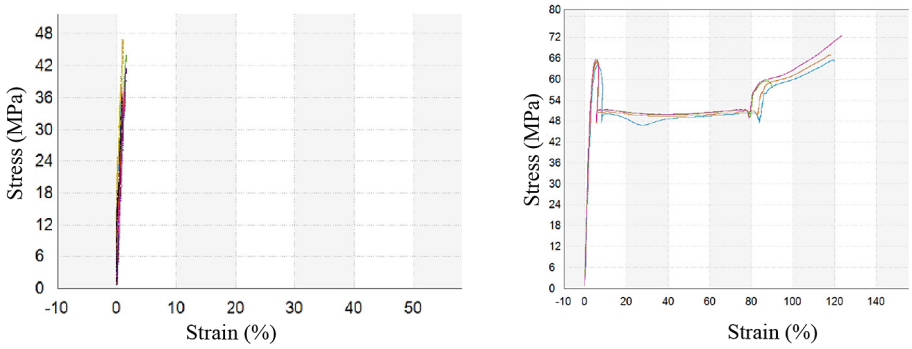

Figure 2. Tensile stress-strain curves for PMMA (a) and PC (b)

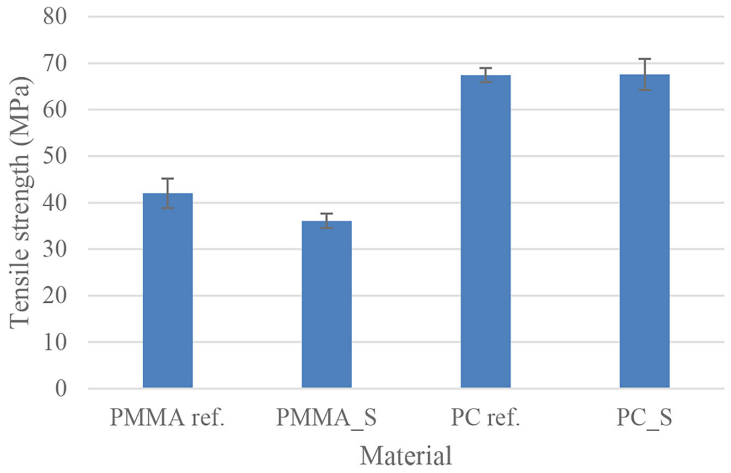

Figure 3. The tensile strength dependence on the test materials

by lower thermal resistance, which has a significant impact on changes in the material characteristics of the material subjected to thermal influence. Figure 4 presents dependence strain at break of function aging time. Figure 4 shows that the highest strain at break characterizes the aged PC_S specimens. PC ref. strain at break is 104.48% (the manufacturer states 124%), which is about 7% lower than PC_S. PMMA specimens' strain at break is below 5% (the manufacturer states 4.5%). Analyzing the graph (Fig. 3) it can be observed that in the case of PMMA_S, there is a smaller spread of results than for reference PMMA. The strain at break is reduced in this case by approximately 7%. The observed differences of strain at break for reference specimens

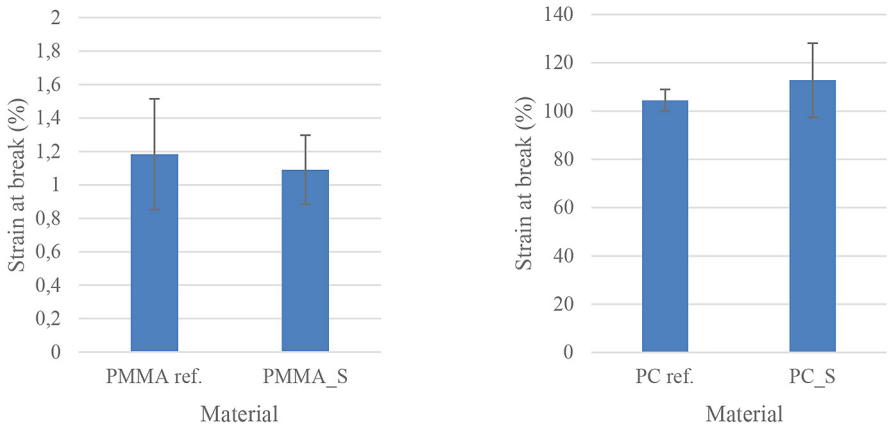

Figure 4. The strain at break dependence on aging process for PMMA (a) and PC (b)

and producer values may be related to the tensile rate, which affects their values, but also with the storage time of the plates.

Three-point flexural test results

Figure 5 presents stress-strain curves determined in tree-point flexural test. Figures 6–8 show the comparison of flexural results taking into account material type and aging time.

Analyzing the graph (Fig. 6), it can be seen that in the case of PMMA specimen has a higher flexural strength, and PMMA_S has a lower flexural strength. The difference between PMMA and PMMA_S is about 15 MPa. It is the result of the aging process. The aged PC_S has a slightly higher flexural strength than the reference specimen – PC but taking into account all the specimens – PC_S has the highest flexural strength. Analyzing the graph (Fig. 7), it can be seen that the unaged specimens – PMMA and PC have a greater flexural strain at break than the aged specimens – PMMA_S and PC_S. The difference in values between PMMA and PMMA_S is approximately 0.5%, similarly for PC and PC_S, which means that the deformation of the tested specimens did not change significantly. However, there is a clear difference between the PC_S and PMMA_S specimens.

Analyzing the graph (Fig. 8), it can be seen that the highest flexural modulus is characterized by unaged specimens – PMMA and the smallest – PC. The graph is descending. The difference between PMMA and PMMA_S is about 200 MPa, making PMMA a material with a higher modulus of elasticity than PMMA_S. The difference between PC and PC_S is less than 100 MPa, making PC_S a material with a slightly higher modulus of elasticity than PC.

Impact test results

Figure 9 shows the results obtained during the impact test. It shows that PC specimens have a higher impact strength, and PMMA specimens

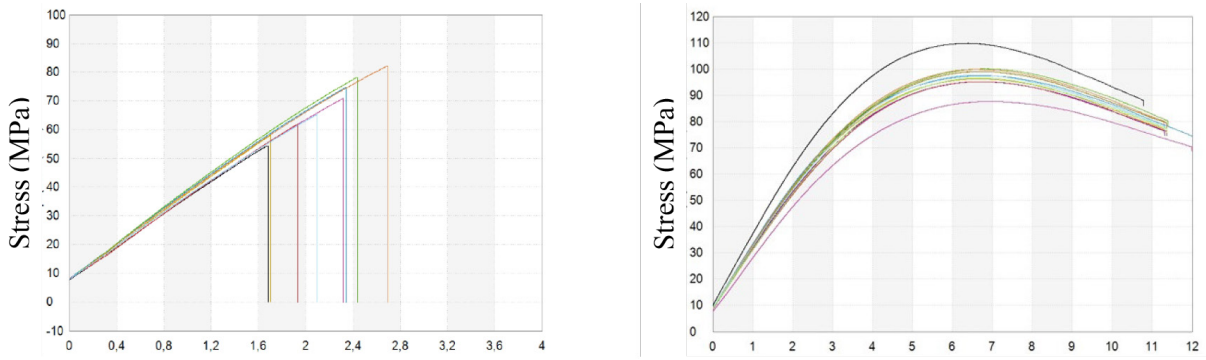

Figure 5. Flexural stress – strain curves for PMMA (a) and PC (b)

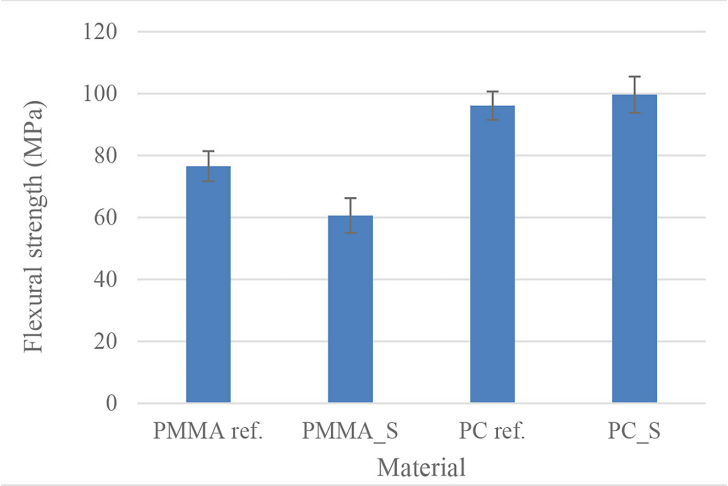

Figure 6. The flexural strength dependence on the test material ang aging process

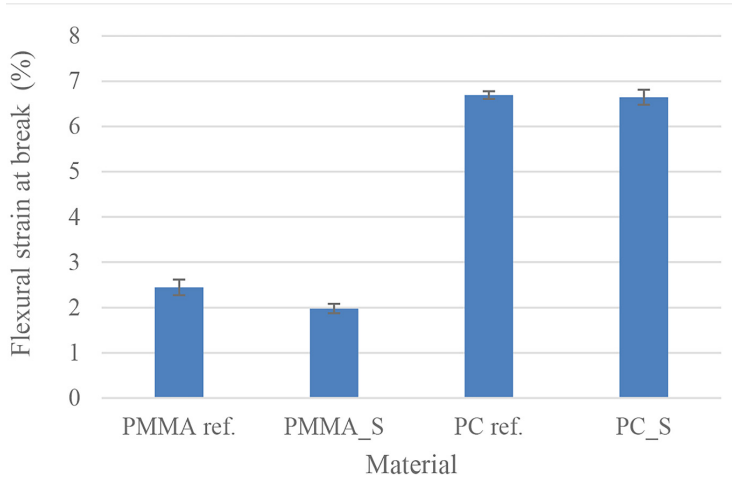

Figure 7. The flexural strain at break dependence on the test material and aging process

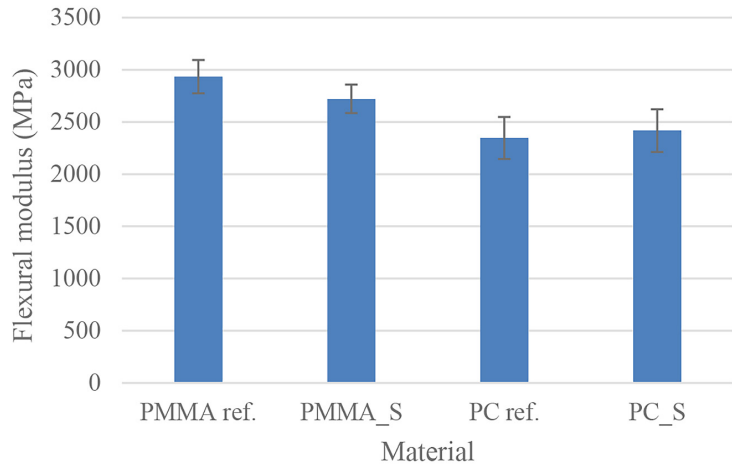

Figure 8. The flexural modulus dependence on the test material and aging process

have a much lower impact strength. In addition, in both cases, the aged specimens have greater impact strength than the reference specimens. The impact strength increased for PMMA and PC, only for PMMA the impact strength increased by 15% and for PC by 4%. This is related to structural changes.

Shore D hardness test results

Figure 10 shows the hardness of tested materials before and after stress corrosion cracking.As a result of exposure of both materials to the synergistic impact of the environment and tensile stresses, a slight increase in PMMA hardness and a slight decrease in PC hardness can be observed (Fig. 10). The increase in PMMA hardness results after 5 days of aging was probably caused by further polymerization of the material in warm water (65±2 ˚C) and the release of residual monomers. On the other hand, PC is one of the hygroscopic plastics, hence we recorded a slight decrease in its hardness.

Density measurement results

Figure 11 shows the average density. As can be observed, the density almost does not change under the influence of test conditions. The presented results are fully repeatable.

Examination with a stereoscopic microscope

Figures 12 and 13 show an example microscopic photo of the structure of specimens after the experiment – specimens PMMA_S. Most small cracks were observed in the specimen mounting area (Fig. 13). This is related to the design of the holders and the method of mounting the specimens. The images show for example microscopic

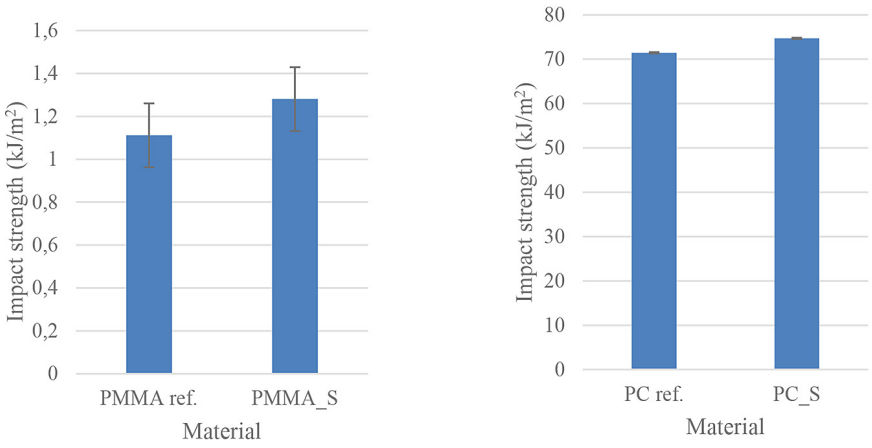

Figure 9. The impact strength dependence on aging process for PMMA (a) and PC (b)

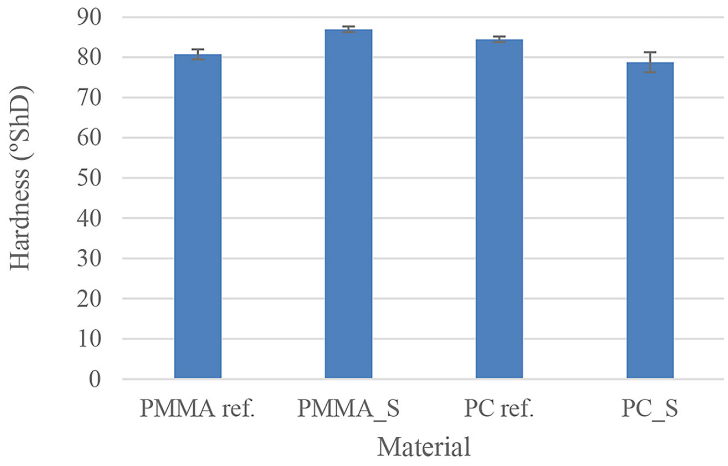

Figure 10. Shore D hardness dependence on the test material and aging process

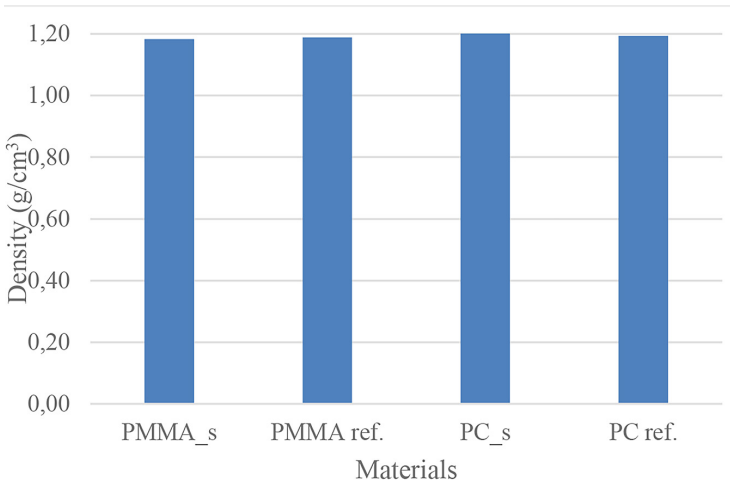

Figure 11. Density dependence on the test material and aging process

photos of the structure of specimens after the experiment – specimens PC_1_S (Fig. 14a, b), PC_2_S (Fig. 15), and PC_3_S (Fig. 16). Comparing the microscopic photos of both materials PMMA and PC, it can be seen that in the case of PMMA, there are fewer cracks on the specimens, and they are smaller in size than those that appeared on PC specimens. This was also confirmed

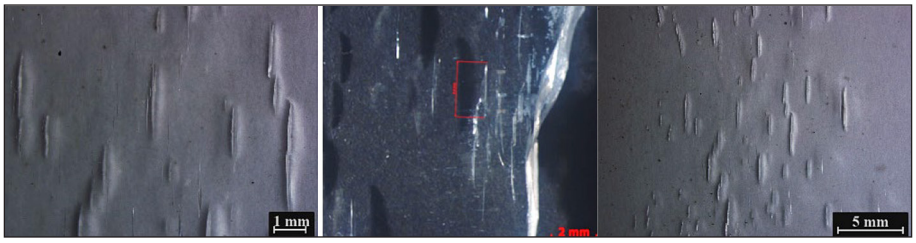

Figure 12. Micrograph of the surface of PMMA_S specimens

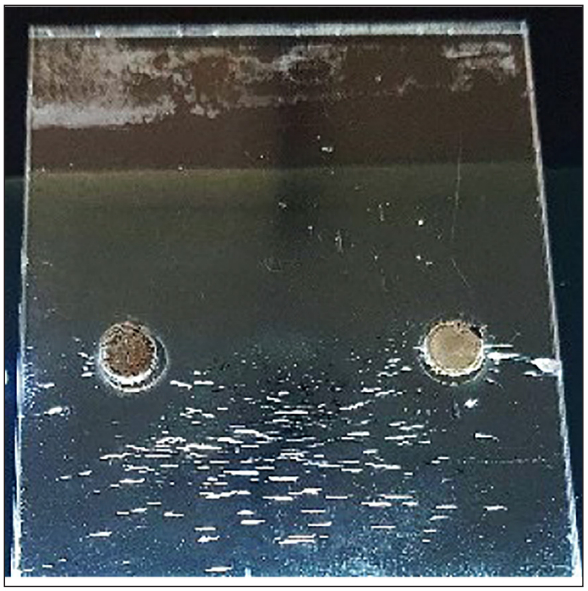

Figure 13. Macroscopic photo of the surface of PMMA_S specimens

in the images of fractures (Fig. 17), where damage can be identified in the case of PMMA as brittle (Fig 17a) and in the case of PC slightly more ductile (Fig. 17b), which results from its moisture absorption in the case of our studies of a saline liquid environment with a neutral pH.

FTIR analysis

Figure 18 presents the IR spectra of the examined materials before and after corrosion tests. The results indicate that the tested materials do not exhibit changes in their chemical backbone (no new peaks were observed after submitting them to aging). However, the specimens undergo significant changes in the peaks' intensity. The PMMA spectra present increasing peaks after corrosion. This is related to the fact that this material exhibits oxidation in seawater causing the formation of

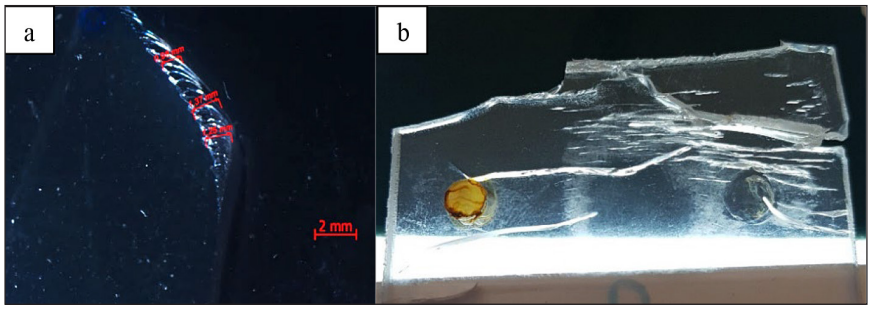

Figure 14. Micrograph (a) and macroscopic photo (b) of the surface of PC_1_S specimens

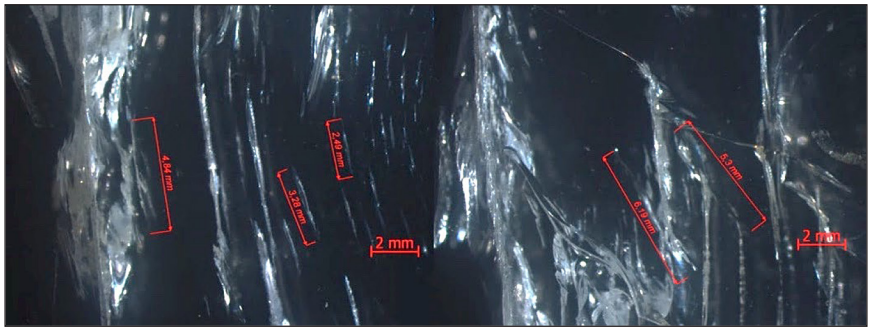

Figure 15. Micrograph of the surface of PC_2_S specimens

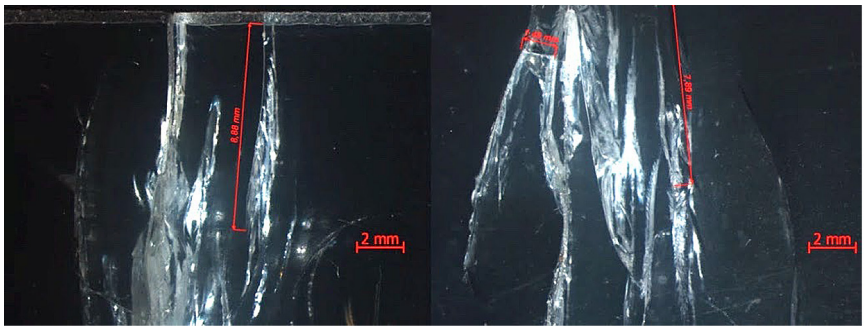

Figure 16. Micrograph of the surface of PC_3_S specimens

Figure 17. Macro photography of the fracture of the specimens PMMA (a) and PC (b)

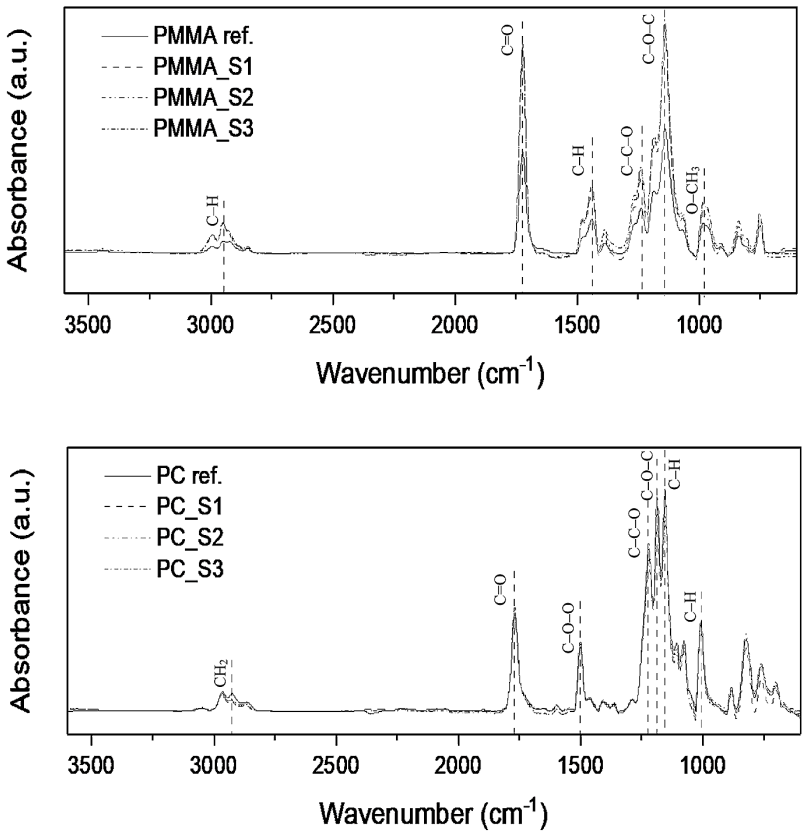

Figure 18. IR spectra of the tested materials: PMMA (a) and PC (b)

dipoles and trapped charges [39]. This in turn increases the intensity of IR polar groups band, i.e., carbonyl group stretching vibration at 1720 cm^{-1}. This explains the higher mechanical behavior of PMMA after aging. The opposite is observed in the PC specimens after aging. A decrease is observed in all characteristic peaks of the material; however, the change in peaks' intensity is minor. This is caused by the rupture of vulnerable bonds and the separation of chains [40]. The alterations in the IR spectra were small, thus the changes in the mechanical properties after aging are minimal.

CONCLUSIONS

Based on the research conducted, it can be concluded:

1. A greater number of corrosion cracks were observed for PMMA. This is related to the functional characteristics. PMMA is less resistant to temperature, which influences the behavior of the tested specimens. These cracks were typical of stress corrosion cracking.
2. Corrosion cracks were arranged perpendicular to the extrusion direction and the greatest density was observed near the handles.
3. The aging process has a significant impact on the properties of materials. In the case of PMMA, a decrease in the tested characteristics is observed, except for impact strength and hardness. The increase in hardness is the result of the aging environment. This is also confirmed by the analysis of FTIR spectra. No changes in surface texture were observed on the PMMA surface, only matting of the surface.
4. PMMA cracks had the character of typical brittle cracks (Fig. 13), and for PC they were ductile cracks (Fig. 14b). For PC, typical stress corrosion cracks appeared only in small areas (Fig. 14b). This behavior of PC specimens is related, among others, to the design of the grip.
5. The duration of exposure to aging conditions on PC was relatively short, so the observed changes are not reliable. However, the analysis of the FTIR spectra showed minimal changes in the increases in the characteristic peaks.
6. The IR spectra revealed major changes in the peaks' intensity of both tested materials. In the case of PMMA the peaks increased after aging due to the formation of dipoles. The opposite is observed for PC, where the characteristic peaks decreased due to chains breaking.

REFERENCES

1. Koch G.H., Tests for Stress-Corrosion, Advanced Materials & Processes/August 2001; 36–38.
2. Guma T.N., Ajayi E.O., Mohammed M.H., Standard techniques of stress corrosion cracking testing: a review, Journal of Newviews in Engineering and Technology (JNET) 2020; 2(1): 58–72.
3. Bieliński, M., Czyżewski, P., Methodology of tests for determining resistance to stress corrosion of plastic components, Modern Engineering 2017; 20–25.
4. Fontana, M.G., Staehle, R.W., Stress Corrosion Cracking in Aircraft Structures. In: ASM Handbook. Corrosion: Environments and Industries. ASM International, Materials Park, OH 2005; 13C.
5. Lim J.K.,13 - Stress corrosion cracking (SCC) in polymer composites, Editor(s): V.S. Raja, Tetsuo Shoji, In Woodhead Publishing Series in Metals and Surface Engineering, Stress Corrosion Cracking, Woodhead Publishing 2011; 485–536C. https://doi.org/10.1533/9780857093769.3.485
6. Megel M., Kumosa L., Ely T., Armentrout D., Kumosa M., Initiation of stress-corrosion cracking in unidirectional glass/polymer composite materials, Compos Sci. Technol. 2001; 61(2): 231–246.
7. Hayes M.D., Edwards D.B., Shah A.R., Fractography in Failure Analysis of Polymers, 2nd Edition – Elsevier 2024.
8. Takafumi Kawaguchi., Hiroyuki N., Keiichi K., Takashi K., Ikuo N. Environmental Stress Cracking (ESC) of Plastics Caused by Non-Ionic Surfactants. Polymer Engineering & Science. 2003; 43: 419–430. https://doi.org/10.1002/pen.10034.
9. Dunn P., Sansom G.F. The stress cracking of polyamides by metal salts. Part I. Metal halides. J. Appl. Polym. Sci. 1969; 13: 1641–1655. https://doi.org/10.1002/app.1969.070130806.
10. Jipa A., Reiter L., Flatt R.J., Dillenburger B. Environmental stress cracking of 3D-printed polymers exposed to concrete, Additive Manufacturing 2022; 58: 103026. https://doi.org/10.1016/j.addma.2022.103026.
11. Solis-Ramos E., Kumosa M., Synergistic effects in stress corrosion cracking of glass reinforced polymer composites, Polymer Degradation and Stability. 2017; 136: 146–157. https://doi.org/10.1016/j.polymdegradstab.2016.12.016.
12. Sridhar, N., Subramanian, C. Stress Corrosion Cracking. In: Subramanian C. (eds) Corrosion for Everybody. Springer, Singapore 2017.
13. Ge H., Le J-L., Mantell S.C., Numerical modeling of stress corrosion cracking of polymers, Engineering Fracture Mechanics 2016; 160: 199–212. https://doi.org/10.1016/j.engfracmech.2016.04.004.
14. Lewis P.R., Environmental stress cracking of polycarbonate catheter connectors, Engineering

Failure Analysis 2009; 16(6): 1816–1824. https://doi.org/10.1016/j.engfailanal.2008.08.026.

15. Almomani A., Mourad A-H.I., Deveci S., Wee J-W., Choi B-H., Recent advances in slow crack growth modeling of polyethylene materials, Materials & Design 2023; 227: 111720. https://doi.org/10.1016/j.matdes.2023.111720.
16. Hejman U., Bjerkén C., Investigation of branching in polycarbonate due to stress corrosion. In: Proceedings 17th European Conference on Fracture, Brno 2008 [Internet]. VUTIUM Brno, Czech Republic; 2008. Available from: https://urn.kb.se/resolve?urn=urn:nbn:se:mau:diva-12472
17. Higuchi, Y. Observation of environmental stress cracking in polymethylmethacrylate by using the chemiluminescence method. Materials Sciences and Applications 2015; 6: 10841088. https://doi.org/10.4236/msa.2015.611107.
18. Arnold J.C. The Effects of Diffusion on Environmental Stress Crack Initiation in PMMA. Journal of Materials Science1998; 33: 5193–5204. http://dx.doi.org/10.1023/A:1004431920449
19. Contino M., Andena L., Rink M., Environmental stress cracking of high-density polyethylene under plane stress conditions, Engineering Fracture Mechanics 2021; 241: 107422, https://doi.org/10.1016/j.engfracmech.2020.107422
20. Ng S.K., Kamaludin M.A., Dear J.P., Blackman B.R., Environmental effects in biaxially orientated Polymethyl Methacrylate, Procedia Structural Integrity 2018; 13: 304–310, https://doi.org/10.1016/j.prostr.2018.12.051
21. Kamaludin M.A., Patel Y., Blackman B.R.K., Williams J.G., Fracture mechanics testing for environmental stress cracking in thermoplastics, Procedia Structural Integrity 2016; 2: 227–234, https://doi.org/10.1016/j.prostr.2016.06.030
22. Andena L., Castellani L., Castiglioni A., Mendogni A., Rink M., Sacchetti F., Determination of environmental stress cracking resistance of polymers: Effects of loading history and testing configuration, Engineering Fracture Mechanics 2013; 101: 33–46, https://doi.org/10.1016/j.engfracmech.2012.09.004
23. Khalifeh, A. Stress corrosion cracking behavior of materials, engineering failure analysis, IntechOpen. Crossref 2020. https://doi.org/10.5772/intechopen.90893.
24. Thuy M., Pedragosa-Rincón M., Niebergall U., Oehler H., Alig I., Böhning M. Environmental stress cracking of high-density polyethylene applying linear elastic fracture mechanics. Polymers 2022; 14(12): 2415. https://doi.org/10.3390/polym14122415
25. Andena L., Rink M., Marano C., Briatico-Vangosa F., Castellani L., Effect of processing on the environmental stress cracking resistance of high-impact polystyrene, Polymer Testing 2016. https://doi.org/10.1016/j.polymertesting.2016.06.017
26. Edvânia T., Suédina S., Rabello, M. Stress cracking and chemical degradation of poly(ethylene terephthalate) in NaOH aqueous solutions. Journal of Applied Polymer Science 2010; 118: 3089–3101. https://doi.org/10.1002/app.32748
27. Altstaedt V., Keiter S., Renner M., Schlarb A. Environmental stress cracking of polymers monitored by fatigue crack growth experiments. Macromol Symp 2004; 214: 31–46. https://doi.org/10.1002/masy.200451004.
28. Turcyl datasheet PMMA.
29. Exolon datasheet.
30. Choi B., Chudnovsky A., Sehanobish K. Stress corrosion cracking in plastic pipes: observation and modelling. International Journal of Fracture 2007; 145(1): 81–88.
31. Bart J.C.J., Additives in polymers. Industrial Analysis and Applications 2005.
32. Fried J.R., Polymer Science and Technology. Third edition 2014; 3–6 / 361–386.
33. Ohama Y., Kobayashi T., Takeuchi K., Nawata K., Chemical resistance of polymethyl methacrylate concrete, International Journal of Cement Composites and Lightweight Concrete 1986; 8(2): 87–91. https://doi.org/10.1016/0262-5075(86)90003-5
34. https://sklep.b.io-space.pl/odpornosc-tworzyw-sztucznych-odpornosc-chemiczna,24,1 08.07.2023
35. https://tools.thermofisher.com/content/sfs/brochures/D20480.pdf, 08.11.2023
36. Van Krevelen D. W., Te Nijenhuis K., Properties of polymers 2009. https://radary.info/temperatura-wody-w-baltyku 06.12.2023.
37. Patent application: P.441463 invention application entitled: Test stand for assessing the impact of a liquid environment on a mechanically loaded sample, especially one tested for corrosion. 2022 (in Polish)
38. Hdiji, S., Namouchi, F., Medhioub, H., Guermazi, H., Guermazi, S., Castellon, J., Toureille, A.. Thermally stimulated depolarization current analysis to the determination of polarization and relaxation parameters in aged PMMA. Mater Sci Eng, 2010; 13: 012018.
39. Redjala, S., Ferhoum, R., Aït Hocine, N. et al. Degradation of polycarbonate properties under thermal aging. J Fail. Anal. and Preven 2019; 19: 536–542. https://doi.org/10.1007/s11668-019-00630-0.